

# Development and Application of Magneto-Optical Microscope Using Polarization-Modulation Technique

Katsuaki Sato<sup>\*,\*\*</sup>, Member  
Takayuki Ishibashi<sup>\*\*\*</sup>, Non-member

**Abstract** Magneto-optical (MO) effect is commonly used not only for an observation of magnetic domain structures, but also for a research of electrical structures in magnetic materials. In addition, distribution of a magnetic flux diverging from a magnetized sample and/or distribution of a current in the sample can be visualized with a help of an MO indicator film placed on the sample. In order to obtain quantitative information of the flux distribution we have developed an MO microscope using a polarization modulation technique. Utilizing the MO microscope with a magnetic garnet film as an indicator we have obtained a quantitative image of current distribution in a superconducting film.

**Keywords** : Magneto-optical effect, Microscope, Polarized light, Polarization modulation, Current distribution, Superconductor

## 1. Introduction

Magneto-optical (MO) microscopes have been used as one of the most significant techniques for an observation of magnetic domain structures in magnetic materials. Recently, this technique attracts great attention as a powerful tool for visualization of invisible phenomena, such as spin-accumulation in nonmagnetic semiconductors<sup>(1,2)</sup>, magnetic flux intrusion in superconductors<sup>(3)-(5)</sup>, etc. MO microscopes have technical advantages such as a short measuring time, a simple instrumental setup compared with other imaging techniques, e.g., a magnetic force microscope (MFM)<sup>(6)</sup>, a superconducting quantum interference device (SQUID) microscope<sup>(7)</sup> and a Hall-probe microscope<sup>(8)</sup>.

However, conventional MO microscopes using a crossed polarizer setup are not suited for quantitative evaluation of the MO rotation and ellipticity, particularly in inhomogeneous samples. In order to overcome the problem, we have developed an MO microscope based on a new concept of polarization modulation technique. This concept is an extension of the modulation MO spectroscopy using photoelastic modulator (PEM), which modulates an optical retardation sinusoidally<sup>(9),(10)</sup>. Since the conventional PEM operates at high frequency of about 50 kHz, the modulation technique is not directly applicable to image observation using CCD sensors. Instead of PEM modulation we utilize a digital modulation method, in which images of the MO rotation and ellipticity are reconstructed from three sequentially captured optical images taken with three different polarization states; i.e., linearly polarized (LP) light, right circularly-polarized (RCP) light and left circularly-polarized (LCP) light<sup>(11)</sup>.

In addition to an evaluation of MO parameters, MO microscopes can be utilized for a visualization of magnetic flux and/or current distribution in superconductors with a help of MO

indicator films such as Bi substituted yttrium iron garnet films<sup>(3)-(5)</sup>. A quantitative magnetic flux image is visualized with a help of the MO indicator film, to which a stray magnetic flux diverging from a superconductor is transferred. A quantitative value of magnitude of the magnetic flux can be calibrated using a magnetic field vs. MO characteristics in the indicator film. As indicator films, we used high quality Bi substituted yttrium iron garnet films with an in-plane magnetization prepared by a metal organic decomposition (MOD) method<sup>(12),(13)</sup>. Combining the MO microscope with this MO indicator film, we have achieved magnetic sensitivity of < 1 mT and spatial resolution of < 1  $\mu\text{m}$ .

## 2. Magnet-Optical Microscope

### 2.1 Polarization Modulation Technique

In our newly-developed system, images of Faraday rotation  $\theta_F$  and Faraday ellipticity  $\eta_F$  can be calculated from three images taken with three different optical polarization states. MO values of each pixel are obtained from equations,

$$\theta_F \approx \frac{1}{2} \left\{ \frac{2I_{LP} - (I_{RCP} + I_{LCP})}{(1 - \eta_F^2)(I_{RCP} + I_{LCP})} \right\}, \dots\dots\dots (1)$$

$$\eta_F \approx \frac{1}{2} \left( \frac{I_{LCP} - I_{RCP}}{I_{LCP} + I_{RCP}} \right), \dots\dots\dots (2)$$

where  $I_{LP}$ ,  $I_{RCP}$  and  $I_{LCP}$  are signal intensities at each pixel point of image data obtained from a CCD camera for LP, RCP and LCP, respectively. Derivation of equations (1) and (2) is described in detail in ref. (11).

In order to obtain images for LCP, LP and RCP sequentially we used a rotatable quarter wave plate in the first stage of development<sup>(14),(15)</sup>. This method, however, took a few tens of second to get one MO image. We improved the response time in the second stage of development; we have made use of a liquid crystal modulator (LCM), by which three polarization images for LCP, LP and RCP can be sequentially measured by only applying to the LCM an AC voltage that is appropriate for each polarization state.

\* Graduate School of Engineering, Tokyo University of Agriculture and Technology, Koganei, Tokyo 184-8588, Japan

\*\* Research Supervisor, Japan Science and Technology Agency, Chiyodaku, Tokyo 102-0075, Japan

\*\*\* Department of Materials Science and Technology, Nagaoka University of Technology, Nagaoka, Niigata 940-2188, Japan

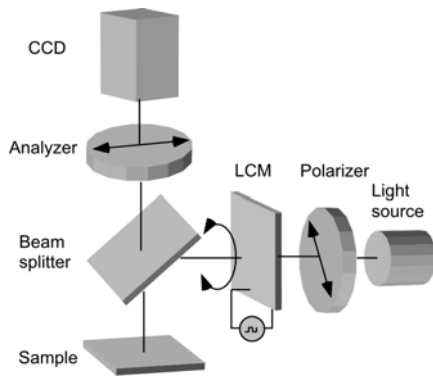


Fig. 1. A schematic drawing of MO microscope using polarization modulation technique.

Figure 1 shows an optical setup of the MO microscope we have developed. This system consists of a light source, a polarizer, a liquid crystal modulator (LCM), a beam-splitter, an analyzer and a CCD camera. An objective lenses with a long working distance (Mitsutoyo G Plan APO  $\times 10$ ,  $\times 50$ ) were employed. Digital images of  $640 \times 480$  pixels were captured from a high speed CCD camera (Hamamatsu, C9300-201) with a 12-bit A-D converter, which allowed directly transfer of 160 digital images/sec to RAM in the computer. As a light source, we used either a halogen-tungsten lamp equipped with interference filters to select wavelength bands between 450 and 650 nm, or a light emitting diode (LED) with a wavelength of 530 nm.

We prepared an LCM employing a commercially available liquid crystal (ZLI-4792) and ITO-coated glass plates. The retardation was varied by an application of AC voltage of 0 - 10 V with a frequency of approximately 100 Hz to the LCM in this experiment. Using this system, MO images can be displayed at a rate of approximately 1 frame/sec using 20 optical images taken with a exposure time of 20 ms<sup>(11)</sup>.

**2.2 MO images of Patterned Garnet Films** Bi, Ga substituted yttrium Iron garnet (YIG) thin film showing a perpendicular magnetization prepared by a metal-organic decomposition (MOD) method<sup>(12)</sup> was used as a sample. In order to investigate the resolution of the magneto-optical contrast, the garnet thin film was patterned into square dot arrays using a photolithography. The size of each dot was  $50 \mu\text{m} \times 50 \mu\text{m}$  in area and 200 nm in thickness, and the separation between dots was 50  $\mu\text{m}$ . Faraday images shown in this section were measured by using a quarter wave plate as a polarization modulator, and Kerr rotation images were measured by using an LCM.

Figures 2 shows images of Faraday rotation (a) and (b), and Faraday ellipticity (c) and (d), of the garnet dot structure measured at the wavelength of 500 nm. These images were reconstructed from three images taken with LP, LCP and RCP using equations (1) and (2) at each pixel point. Right (Figs. 2(a) and 2(b)) and left images are those corresponding to opposite remanent states after magnetizing toward opposite directions by the saturating field. A reversal of the magnetic contrast between the glass and the garnet portions are clearly observed corresponding to a magnetization reversal. In addition to the magnetic contrast, quantitative values of  $\theta_F$  and  $\eta_F$  can be obtained at any pixel on the image. Therefore, the present technique provides a quantitative magnetic contrast even in inhomogeneous samples consisting of different portions

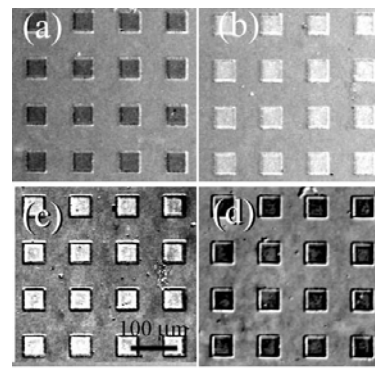


Fig. 2. (a) and (b) are Faraday rotation images, and (c) and (d) Faraday ellipticity images with opposite remanent states. A rotation image and an ellipticity image were obtained from same images for LP, LCP and RCP.

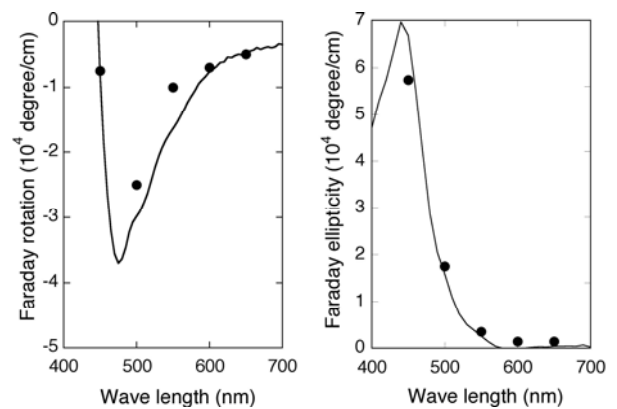


Fig. 3. (a) Faraday rotation and (b) Faraday ellipticity spectrum. Solid curves shows spectrum measured by a conventional spectrometer for continuous film, and dots show data measured by the MO microscope..

with different transmittance, for which the conventional crossed polarizer method fails to provide quantitative MO values, since the contrast is given only as a difference in optical intensities in the latter system. The values of  $\theta_F$  and  $\eta_F$  measured with wavelength of 450 – 650 nm are plotted in Figure 3 together with solid lines showing data of a continuous film measured by an MO spectrometer. As observed in the figure, MO values measured by the MO microscope are found to show a remarkable agreement with those measured by the MO spectrometer.

Since most magnetic materials are not transparent, the measurement of Kerr effect is important for practical use. Figure 4 shows magnetic field-dependences of Kerr rotation at wavelength of 500 nm for a garnet dot and a glass substrate shown by an inset. Once MO images are acquired for a sequence of magnetic field swinging between negative and positive magnetic saturation, hysteresis curves at any pixel point can be visualized only by clicking at the point. As shown in Figure 4, a clear hysteresis loop is observed at the patterned garnet position, while no signal was observed at the glass substrate position.

A spatial resolution  $d$  of the MO image obtained using the optical microscope system can be expressed by a formula,  $d = 0.6\lambda / NA$ , where  $\lambda$  is a wavelength and  $NA$  is a numerical aperture of the objective lens employed. In the present study, the spatial resolution is estimated to be approximately 0.5  $\mu\text{m}$  using a

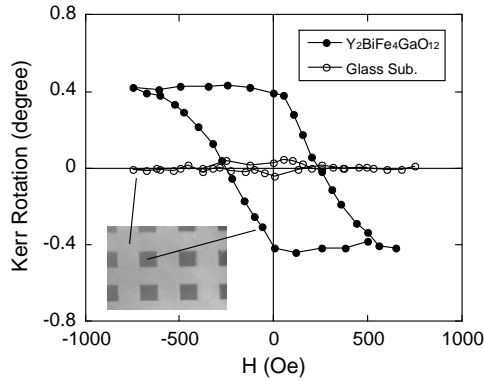


Fig. 4. Magnetic field dependences of Kerr rotation for the garnet dot and the glass substrate.

value  $NA=0.5$  for the objective lens employed in the experiment.

The sensitivity in MO images was mainly limited by a shot noise generated in the CCD device. We carried out two kinds of averaging procedures in order to improve the signal to noise ratio (SNR): One was an averaging by accumulation of repeated data at each pixel point, and the other was an averaging over 9 pixel points including 8 pixels surrounding the pixel of concern. An averaging over 100 and 1000 images gave us a noise with a standard deviation of  $0.008^\circ$  and  $0.005^\circ$  for the angle of rotation.

### 3. Magnetic Imaging

**3.1 MO indicator films** The MO microscope combined with an MO indicator film allows us to observe a magnetic flux distribution and/or a current distribution in materials even if the sample itself does not show any MO effect. As described before, we used as an MO indicator a Bi-substituted iron garnet film,  $Y_2BiFe_5O_{12}$  (Bi:YIG) with an in-plane anisotropy prepared by the MOD method. The MOD method is favorable not only for the homogeneity of a thin film, the controllability of composition, and the formation of large area, but for the good productivity, since the method makes use of a quite simple procedure, i.e. a spin-coating of solution containing constituent elements and an annealing. Details of preparation of garnet films by the MOD method have been described in ref.(12). Pt mirror layer with a thickness of 100 nm was deposited on the garnet film by a magnetron sputtering method in order to obtain high reflectivity and to avoid scattering of the light due to the pattern fabricated on the sample.

Figure 5 shows a magnetic field-dependence of Faraday rotation in the Bi:YIG film with a mirror layer measured by the MO microscope from substrate side using a light of 500 nm in wavelength. It shows that the film has an easy-axis of magnetization in-plane direction and the Faraday rotation is linearly dependent on the magnetic field, reaching a saturation value at the magnetic field of approximately 1 kOe. The magnitude of magnetic flux for each pixel in an MO image can be calibrated using this relationship.

Next, we show that the MOD-grown garnet film is more suitable for use as an MO-indicator than a liquid phase epitaxial (LPE) film. Figures 6(a) and 6(b) show magnetic flux images of a superconducting Nb film measured with an indicator of the LPE film and the MOD film, respectively. The size of the Nb film was  $0.9 \text{ mm} \times 0.9 \text{ mm}$  in area and 200 nm in thickness. The temperatures of measurement was 4 K, sufficiently lower than the

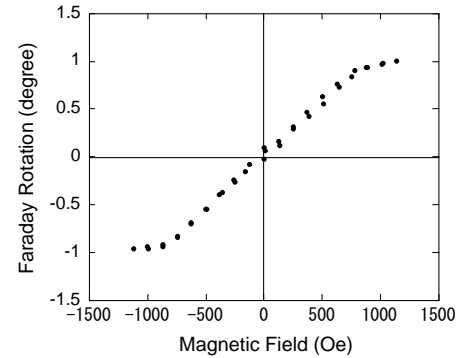


Fig. 5. Magnetic field dependence of Faraday rotation of Bi:YIG film measured at a wavelength of 500 nm.

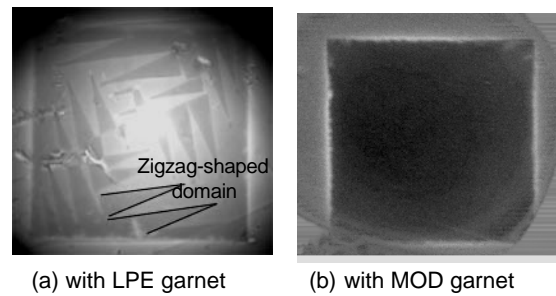


Fig. 6. Magneto-optically observed images of magnetic flux from a superconducting Nb using (a) an LPE film and (b) an MOD film as an MO indicator.

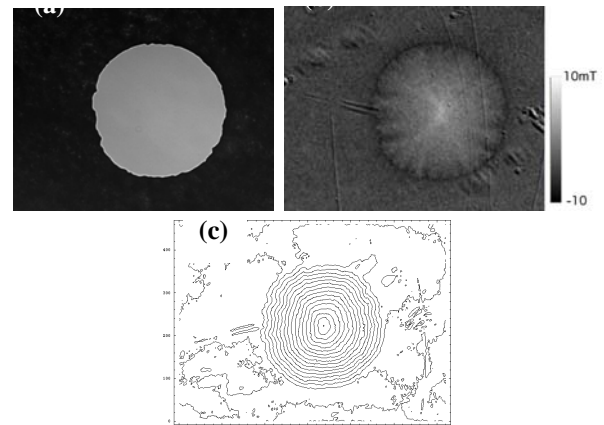


Fig. 7. (a) An optical image of  $MgB_2$  circular pattern with a diameter of  $500 \mu\text{m}$  without an indicator and (b) a magneto-optically observed image of magnetic flux of the  $MgB_2$  pattern using MOD garnet indicator. (c) A current flow image of the  $MgB_2$  pattern deduced from the MO image shown in (b).

critical temperature ( $\sim 9 \text{ K}$ ) of the Nb film. The images in Figures 6 (a) and 6 (b) are showing Meissner state under an applied magnetic field of 16 and 26 Oe, respectively. Thickness of the LPE grown garnet and the MOD grown garnet used in this experiment was  $2 \mu\text{m}$  and  $800 \text{ nm}$ , respectively. It was found that with a use of the LPE garnet the image suffered zigzag-shaped magnetic domains appearing in the garnet, while with the MOD garnet no such domain structure appeared and allowed us to observe the flux distribution clearly. It is thus concluded that the Bi:YIG films grown by MOD method is suitable for MO imaging. Further details have been described in Ref. 13.

### 3.2 MO IMAGES OF SUPERCONDUCTORS

MO images of superconducting  $\text{MgB}_2$  film was measured by the MO microscope using the Bi:YIG film directly covering the sample placed in a cryostat with an electro-magnet. The  $\text{MgB}_2$  film of 100 nm in thickness was grown by a molecular beam epitaxy (MBE) method<sup>(16)</sup> and was patterned into circular shape of 500  $\mu\text{m}$  in diameter. MO images were measured at 3.9 K with different magnetic fields after zero-field cooling.

Figures 7(a) shows an optical image of the patterned  $\text{MgB}_2$ , while 7(b) shows an MO image of a remanent state after application of magnetic field of 735 Oe. A magnetic flux gradient is clearly observed in the latter. The contrast in the image corresponds to an amount of magnetic flux intruding into the superconductor. From the MO image, a current distribution can be calculated taking into account the Biot-Savart law. Figure 7(c) shows a current flow image calculated using the convolution theorem<sup>(17)</sup>, where the contour line indicates a current flow and the density of contour lines corresponds to a current density. The current density deduced from the figure amounts to as high as  $6 \times 10^7 \text{ A/cm}^2$ , which is consistent with an electrical measurement.

### 4. Conclusion

We have developed an MO microscope using the polarization modulation technique. Quantitative MO imaging were demonstrated for patterned Bi,Ga:YIG films, and spectra and hysteresis measurements were also demonstrated. In addition, quantitative MO imaging combined with MO indicator films was useful technique to measure magnetic flux images in samples showing no MO effects. Magnetic flux distribution and current flow images were successfully obtained for superconducting patterns.

### Acknowledgement

This work has been supported in part by the Grant-in-Aid for Scientific Research, Basic Research B (No.16360003) from the Japan Society for Promotion of Science. We thank Dr. H. Shibata of NTT basic Research Laboratory and Prof. M. Naito of Tokyo Univ. of Agriculture and Technology for providing  $\text{MgB}_2$  samples. We also thank Prof. T. H. Johansen and Dr. J. I. Vestgård of Univ. of Oslo for the calculation of current images. (Manuscript received December 25, 2007, revised April 9, 2008)

### References

- (1) S. A. Crooker, M. Furis, X. Lou, C. Adelman, D. L. Smith, C. J. Palmström, P.A. Crowell: "Imaging Spin Transport in Lateral Ferromagnet/Semiconductor Structures", *Science*, Vol.309, pp.2191-2195 (2005).
- (2) M. Yamanouchi, D. Chiba, F. Matsukura, and H. Ohno: "Current-induced domain-wall switching in a ferromagnetic semiconductor structure", *Lett. Nature*, Vol.428, pp.539-542 (2004).
- (3) S. Gotoh, N. Koshizuka, M. Yoshida, M. Murakami, and S. Tanaka: "Direct Observation of Flux Behavior in High-Tc Oxide Superconductors Using The Faraday Effect of Iron Garnet Films", *Jpn. J. Appl. Phys.*, Vol.29, L1083-L1085 (1990).
- (4) M. V. Indenbom, N. N. Kolesnikov, M. P. Kulakov, I. G. Naumenko, V. I. Nikitenko, A. A. Polyanskii, N. F. Vershinin, and V. K. V. Vlasov: "Direct study of magnetic flux penetration and trapping in HTSC", *Physica C*, Vol.166, pp.486-496 (1990).
- (5) P.E. Goa, H. Hauglin, Å.A.F. Olsen, M. Bzilevich, and T.H. Johansen: "Magneto-optical imaging setup for single vortex observation", *Rev. Sci. Instrum.*, Vol.74, pp. 141-146 (2003).
- (6) Y. Martin, D. Rugar, and H. K. Wickramasinghe: "High-resolution magnetic imaging of domains in TbFe by force microscopy", *Appl. Phys. Lett.*, Vol.52, 244-246 (1988).
- (7) J. R. Kirtley, M. B. Ketchen, K. G. Stawiasz, J. Z. Sun, W. J. Gallagher, S. H.

Blanton, and S. J. Wind: "High-resolution scanning SQUID microscope", *Appl. Phys. Lett.*, Vol.66, pp.1138-1140 (1995).

- (8) A. M. Chang, H. D. Hallen, L. Harriott, H. F. Hess, H. L. Kao, J. Kwo, R. E. Miller, R. Wolfe, and J. van der Ziel, and T. Y. Chang: "Scanning Hall probe microscopy", *Appl. Phys. Lett.*, Vol.61, pp.1974-1976 (1992).
- (9) K. Sato: "Measurement of Magneto-Optical Kerr Effect Using Piezo-Birefringent Modulator", *Jpn. J. Appl. Phys.*, Vol.20, pp.2403-2409 (1981).
- (10) K. Sato, H. Hongu, H. Ikekame, Y. Tosaka, M. Watanabe, K. Takanashi, H. Fujimori: "Magneto-optical Kerr Spectrometer for 1.2-5.9 eV Region and its Application to FePt/Pt Multilayers", *Jpn. J. Appl. Phys.*, Vol.32, pp.989-995 (1993).
- (11) T. Ishibashi, Z. Kuang, S. Yufune, T. Kawata, M. Oda, T. Tani, Y. Iimura, Y. Konishi, K. Akahane, X. R. Zhao, T. Hasegawa, and K. Sato: "Magneto-Optical Imaging Using Polarization Modulation Method", *J. Appl. Phys.*, Vol.100, 093903 (2006).
- (12) T. Ishibashi, A. Mizusawa, M. Nagai, S. Shimizu, K. Sato, N. Togashi, T. Mogi, M. Houchido, H. Sano, and K. Kuriyama: "Characterization of epitaxial  $(\text{Y,Bi})_3(\text{Fe,Ga})_5\text{O}_{12}$  thin films grown by metal-organic decomposition method", *J. Appl. Phys.*, Vol.97, 013516 (2005).
- (13) T. Ishibashi, T. Kawata, T. H. Johansen, J. He, N. Harada, and K. Sato: "Magneto-optical Indicator Garnet Films Grown by Metal-organic Decomposition Method", *J. Mag. Soc. Jpn.*, Vol. 31 (2008) to be published.
- (14) X. R. Zhao, N. Okazaki, Y. Konishi, K. Akahane, Z. Kuang, T. Ishibashi, K. Sato, H. Koinuma, and T. Hasegawa: "Magneto-optical Imaging for High-Throughput Characterization of Combinatorial Magnetic Films", *Appl. Surface Science*, Vol. 223, pp.73-77 (2004).
- (15) X.R. Zhao, W.-Q. Lu, S. Okazaki, Y. Konishi, K. Akahane, T. Ishibashi, K. Sato, Y. Matsumoto, H. Koinuma, T. Hasegawa: "High-throughput characterization of  $\text{Bi}_x\text{Y}_{3-x}\text{Fe}_5\text{O}_{12}$  combinatorial thin films by magneto-optical imaging technique", *Applied Surface Science*, Vol.252 pp.2628-2633 (2006).
- (16) K. Ueda and N. Naito: "In-situ growth of superconducting  $\text{MgB}_2$  thin films by molecular-beam epitaxy", *J. Appl. Phys.*, Vol.93, pp.2113-2120 (2003).
- (17) Ch. Jooss, R. Warthmann, A. Forkl and H. Kronmüller: "High-resolution magneto-optical imaging of critical currents in  $\text{YBa}_2\text{Cu}_3\text{O}_{7-x}$  thin films", *Physica C*, Vol.299, pp.215-230 (1998).

**Katsuaki Sato** (Member) received the B. E., M.E., and Doctor of Eng.



Degree from Kyoto University, Kyoto, Japan, in 1964, 1966, and 1978, respectively. He joined Japan Broadcasting Corporation in 1966. He joined Tokyo University of Agriculture and Technology as an associate professor in 1984, and promoted to a professor in 1989, and assumed a vice president from 2005 to 2007. He is presently a professor in Graduate School of Engineering, Tokyo University of Agriculture and Technology, and a research supervisor of PRESTO Project, Japan Science and Technology Agency. His research includes growth and characterization of magnetic materials, multinary semiconductors and superconducting materials, and magneto-optics. He is a fellow member of the Japan Society of Applied Physics.



**Takayuki Ishibashi** (Nonmember) received the B. E., M.E., and Doctor of Eng. degree from University of Tsukuba, Ibaraki, Japan, in 1991, 1993, and 1995, respectively. He was an assistant professor of Tokyo University of Agriculture and Technology from 1995 to 2007. He is presently an associate professor in Department of Materials Science and Technology, Nagaoka University of Technology. His research includes thin film growth of magnetic materials and superconducting materials, and magneto-optical imaging. He is a member of the Japan Society of Applied Physics, the Magnetic Society of Japan, the Physical Society of Japan, and the Ceramics Society of Japan.